3062 *Chem. Mater.* **2009,** *21,* 3062–3071
DOI:10.1021/cm803060d

CHEMISTRY OF MATERIALS
Article

Ionically Self-Assembled Polyelectrolyte-Based Carbon Nanotube Fibers

Sandeep Razdan,[†] Prabir K. Patra,*[,‡] Swastik Kar,[†,⊥] Lijie Ci,[‡] Robert Vajtai,[‡] Ákos Kukovecz,[§] Zoltán Kónya,[§] Imre Kiricsi,[§] and Pulickel M. Ajayan*[,‡]

[†]*Department of Materials Science & Engineering, Rensselaer Polytechnic Institute, Troy, New York 12180,* [‡]*Department of Mechanical Engineering and Materials Science, Rice University, Houston, Texas 77005, and* [§]*Department of Applied and Environmental Chemistry, University of Szeged, Rerrich Béla tér 1, 6720 Szeged, Hungary.* [⊥]*Currently at Department of Physics, Rensselaer Polytechnic Institute, Troy, New York 12180*

Received November 20, 2008. Revised Manuscript Received May 25, 2009

We present a process for synthesizing ionically self-assembled polyelectrolyte-complex-based carbon nanotube fibers using a simple noncovalent stabilization of carbon nanotube aqueous dispersions where no surface functionalizations of the nanotubes were necessary. The polyelectrolyte-carbon nanotube composite fibers have mechanical, electrical and chemical properties which make them a choice of materials in applications such as biosensors, chemical electrodes or flexible electronics. The fibers showed reasonable strength and conductivity as high as 45 S/cm for single-walled carbon nanotubes and 80—90 S/cm for multiwalled carbon nanotubes, due to the presence of an interconnected network of carbon nanotubes embedded inside the fibers. Fiber formation was demonstrated for a variety of strong polyelectrolyte combinations, including a conductive fiber matrix consisting of poly (ethylenedioxythiophene) (PEDOT), with the presence of nanotubes causing a 2 orders of magnitude increase in the conductivity of the base polymer. The self-assembled polyelectrolyte-carbon nanotube fibers have potential applications in biosensing and flexible electronics.

1. Introduction

Polyelectrolytes are polymers that carry resident chargeable groups within their intrinsic molecular structure.[1,2] Examples of such polymers encompass naturally occurring structures as DNA, amino acids,[1] as well as synthetically prepared polymers such as chitosan and polystyrenesulfonate (PSS).[1] The distinctive properties of these polymers arising from surface-charge-based interactions and their biocompatible nature make them useful for a variety of applications such as viscosity modifiers, flocculants,[3,4] drug delivery systems, biosensors,[5−7] and membranes.[8,9] Polyelectrolyte complexes (PEC) are formed when two oppositely charged polyelectrolytes interact with each other to neutralize some or all of the resident charges on the macromolecular chains.[1] A polyelectrolyte complex may be soluble in the solvent medium, or exist in a phase-separated form of a precipitate.[1,10,11] Previous literature has shown the possibility of formation of fibrous structures from self-assembly of certain polyelectrolyte complex precipitates.[12−18] Yamamoto et al. reported in 2000 the formation of microstructures such as mircocapsules and fibers, by using biocompatible polyelectrolytes such as chitosan and poly (α, L-glutamic acid) (PLG).[14] These polyelectrolytes can be spun into fibers and collected continuously. These structures have potential use as drug delivery systems, biosensors, and electrochemical electrodes.[12−18]

Our work focuses on understanding the carbon nanotube−polyelectrolyte self-assembled complexation process to produce novel layered fibrous structures. The remarkable electrical[19−25] and mechanical

*Corresponding author. P.M.Ajayan, E-mail: ajayan@rice.edu (P.M.A.); prabir@rice.edu (P.K.P.).

(1) Hara, M. Polyelectrolytes; Marcel Dekker, Inc.: New York, 1993.
(2) Gray, F. M. Solid Polymer Electrolytes; VCH: Weinheim, Germany, 1991.
(3) Whipple, W. L.; Maltesh, C. *Langmuir* **2000**, 16, 3124.
(4) Li, D.; Zhu, S.; R. Pelton, R. H.; Spafford, M. *Colloid Polym. Sci.* **1999**, 277, 108.
(5) Li, Y.; Su, X.; Ye, Q. A *J. Appl. Polym. Sci.* **2002**, 86, 2067.
(6) Shalaby, S. E.; Al-Balakocy, N. G.; Abo El-Ola, S. M. *J. Appl. Polym. Sci.* **2007**, 104, 3788.
(7) Yu, A.; Caruso, F. *Anal. Chem.* **2003**, 75, 3031.
(8) Krasemann, L.; Tieke, B. *J. Membr. Sci.* **1998**, 150(1), 23.
(9) Miller, M. D.; Bruening, M. L. Langmuir, **2004**, 26, 11545.
(10) Webster, L.; Huglin, M. B.; Robb, I. D. *Polymer* **1997**, 38(6), 1373.
(11) M. Mende, M.; Petzold, G.; Buchhammer, H-, M. *Colloid Polym. Sci.* **2002**, 280, 342.
(12) Ohkawa, K.; Takahashi, Y.; Yamada, M.; Yamamoto, H. *Macromol. Mater. Eng.* **2001**, 286, 168.
(13) Yamamoto, H.; Senoo, Y. *Macromol. Chem. Phys.* **2000**, 201, 84.
(14) Ohkawa, K.; Takahashi, Y.; H. Yamamoto, H. *Macromol. Rapid Commun.* **2000**, 21, 223.
(15) Yamamoto, H.; Horita, C.; Senoo, Y.; Nishida, A.; Ohkawa, K. *J. Appl. Polym. Sci.* **2001**, 79, 437.
(16) Hachisu, M.; Ohkaw, K.; Yamamoto, H. *Macromol. Biosci.* **2003**, 3, 92.
(17) Liao, I.-C.; Wan, A. C. A.; Yim, E. K. F.; Leong, K. W. *J. Controlled Release* **2005**, 104, 347.
(18) Wan, A. C. A.; Liao, I.-C.; Yim, E. K. F.; Leong, K. W. *Macromolecules* **2004**, 37, 7019.
(19) Ajayan, P. M. *Chem. Rev.* **1999**, 99, 1787.
(20) Ebbesen, T. W.; Lezec, H.; Hiura, H.; Bennett, J. W.; Ghaemi, H. F.; Thio, T. *Nature* **1996**, 382, 54.
(21) Saito, R.; Dresselhaus, M. S.; Dresselhaus, G. Physical Properties of Carbon Nanotubes; World Scientific: New York, 1998.
(22) Wei, B. Q.; Vajtai, R.; Ajayan, P. M. *Appl. Phys. Lett.* **2001**, 79(8), 1172.
(23) Carroll, D. L.; Redlich, P.; Blasé, X.; Charlier, J. C.; Curran, S.; Ajayan, P. M.; Roth, S.; Ruhle, M. Phys. Rev. Lett., **1998**, 81, 2332.
(24) Czerw, R.; Terrones, M.; Charlier, J. C.; Blasé, X.; Foley, B.; R. Kamalakaran, R.; Grobert, N.; Terrones; Tekleab, D.; Ajayan, P. M.; Blau, W.; Ruhle, M.; D. L. Carroll, D. L. *Nano Lett.* **2001**, 1, 457.
(25) Rao, A. M.; Eklund, P. C.; Bandow, S.; Thess, A.; Smalley, R. E. *Nature* **1997**, 388, 257.

 Published on Web 06/18/2009

properties[26−31] of carbon nanotubes make them useful for a variety of applications such as chemical and biological sensors,[32−34] interconnects,[35] electrodes,[36] supercapacitors,[37] and fuel cells.[38] Nanotubes have also been used as fillers for polymer composites;[39−42] however, conventional techniques to prepare nanotube based composites require various functionalization schemes in order to obtain a good interface between the polymer and the nanotube surface.[43] Our technique utilizes the self-assembly of polyelectrolyte complex systems via a simple water-based process requiring no functionalization of nanotube surface, to prepare unique nanotube containing multicomponent composites combining the useful properties of both nanotubes and polyelectrolytes. Besides providing an alternative route for fabrication of carbon nanotube-based fibers, this process also delineates the structure−property relationships of nanotube-based composites containing complex charge-carrying polymer systems that have potential applications in biosensing, ion-selective membranes, and fuel cells.

2. Experimental Methods

Single-walled carbon nanotubes (SWNTs), produced via the HiPCO process, were purchased from Carbon Nanotechnologies Inc. Multiwalled carbon nanotubes (MWNTs) synthesized using a catalytic chemical vapor deposition (CCVD) process[44] were produced at University of Szeged, Hungary. The as-produced MWNTs were oxidized in 0.1 M H_2SO_4 and $KMnO_4$ with a resultant purity of more than 95% after the oxidation process. Sodium salt of polystyrenesulfonate (PSS) of molecular weight 70 000 was purchased from Sigma Aldrich. Polydiallyldimethylammonium chloride (PDDA) was purchased from Sigma Aldrich in molecular weight range of 400 000−500 000. Both PSS and PDDA were used as the primary system for study of formation of polyelectrolyte complexes based on carbon nanotubes. Other polyelectrolytes also used in the study were poly(3,4-ethylendioxythiophene) (PEDOT), a conductive polymer obtained as a polymer mixture with PSS; chitosan (high molecular weight, >75% deacetylated), a biopolymer produced from deacetylation of chitin; and poly (L-glutamic acid) (PLG) (sodium salt, molecular weight 50 000−100 000), all of which were purchased from Sigma Aldrich.

A Cole-Parmer ultrasonicating bath (20 kHz) was used in conjunction with a Sonics Vibracell ultrasonicating probe (20−30% amplitude, 500 W) in order to assist dispersion of nanotubes. SEM characterization was carried out using a JEOL JSM-6330F instrument equipped with an Oxford EDS detector. Optical microscopy was carried out using an Olympus BH2 optical microscope with a 100× objective and an attached camera for time lapse photography. Thermogravimetric analysis was carried out using a Mettler Toledo 851e thermogravimetric analyzer using a temperature range of 25−1000 °C with a heating rate of 10 °C/min. FTIR spectroscopy was performed using a Perkin-Elmer Spectrum One instrument.

Uniaxial tensile testing of the fibers was carried out using the Instron 5845 instrument. The fiber ends were mounted on a small piece of paper (cut at the center) using epoxy, giving a gauge length of around 10 mm. These were then mounted on the Instron machine and tested at a constant rate of traverse of 0.03 mm min^{-1}.

Electrical properties of the fibers were measured by mounting on a substrate as shown in the inset in Figure 11, consisting of copper prongs regularly spaced apart by 2 mm, using silver paint as the electrical contact. Both 2 probe and 4 probe measurements were carried out using a Keithley 2400 sourcemeter for currents ranging from 100 nA to 100 μA.

3. Results and Discussion

3.1. Fiber Synthesis. To prepare carbon nanotube based fibers, both single- and multiwalled carbon nanotubes were dispersed in an aqueous solution of 1 wt % PSS using ultrasonication, in three different concentrations of 0.1, 0.5, and 1 wt %. PSS is known to be an effective dispersant of nanotubes in water via noncovalent stabilization.[45] The dispersion of nanotubes in PSS solution is attributed to a polymer "wrapping" mechanism where the hydrophobic portions of the polymer chain tend to cover the nanotube surface forming uniform monolayers and the polar hydrophilic part interacts with water to effectively deaggregate nanotube bundles.[45]

Dispersion of carbon nanotubes in aqueous PSS solution was assisted via the ultrasonication process, by alternate treatments using an ultrasonication bath (20 kHz) and an ultrasonicaing tip (30% amplitude) each for an hour. This helped to debundle nanotube aggregates thereby making larger amount of surface area available for interaction with PSS, without causing too much damage to the nanotube surface. Figure 1 shows scanning

(26) Ruoff, R.; Lorents, D. C. *Carbon* **1995**, 33(7), 925.
(27) Yakobson, B. I.; Brabec, C. J.; Bernholc, J. *Phys. Rev. Lett.* **1996**, 76(14), 2511.
(28) Yu, M. F.; Files, B. S.; Arepalli, S.; Ruoff, R. S. *Phys. Rev. Lett.* **2000**, 84, 5552.
(29) Krishnan, A.; Dujardin, E.; Ebbesen, T. W.; Yianilos, P. N.; M. J. Treacy, M. J. *Phys. Rev. B* **1998**, 58, 14013.
(30) Wong, E. W.; Sheehan, P. E.; Lieber, C. M. *Science* **1997**, 277, 1971.
(31) Langer, L.; Bayot, V.; Grivei, E.; Issi, J. P.; Olk, C. H.; Stockman, L.; Van Haesendonck, C.; Bruynseraede, Y. *Phys. Rev. Lett.* **1996**, 76, 479.
(32) Kong, J.; Franklin, N. R.; Zhou, C.; Chapline, M. G.; Peng, S.; Cho, K.; Dai, H. *Science* **2000**, 287, 622.
(33) Sotiropoulou, S.; Chaniotakis, N. A. *Anal. Bioanal. Chem.* **2003**, 375(1), 103.
(34) Chen, R. J.; Bangsaruntip, S.; Drouvalakis, K. A.; Kam, N.W. S.; M. Shim, M.; Li, Y.; Kim, W.; Utz, P. J.; Dai, H. *Proc. Natl. Acad. Sci.* **2003**, 100(9), 4984.
(35) Kreupl, F.; Graham, A. P.; Duesberg, G. S.; Steinhoegl, W.; Liebau, M.; Unger, E.; Hoenlein, W. *Microelectron. Eng.* **2002**, 64, 399.
(36) Kruger, M.; Widmer, I.; T. Nussbaumer, T.; Buitelaar, M.; Schonenberger, C. *New J. Phys.* **2003**, 5, 138.
(37) Talapatra, S.; Kar, S.; Pal, S. K.; Vajtai, R.; Ci, L.; Victor, P.; Shaijumon, M. M.; Kaur, S.; O. Nalamasu, O.; Ajayan, P. M. *Nat. Nanotechnol.* **2006**, 1, 112.
(38) Kim, D. W.; Lee, J. S.; Lee, G. S.; Overzet, L.; Kozlov, M.; Aliev, A. E.; Park, Y. W.; Yang, D. J. *J. Nanosci. Nanotechnol.* **2006**, 6, 3608.
(39) Barrera, E. V. *JOM* **2000**, 52, 38.
(40) Park, C.; Ounaies, Z.; Watson, K. A.; Crooks, R. E.; Smith, J.; Lowther, S. E.; J. Connell, J. W.; Siochi, E. J.; Harrison, J. S.; St. Clair, T. L. *Chem. Phys. Lett.* **2002**, 364, 303.
(41) Safadi, B.; Andrews, R.; Grulke, E. A. *J. Appl. Polym. Sci.* **2002**, 84, 2660.
(42) Shaffer, M. S. P.; Windle, A. H. *Adv. Mater.* **1999**, 11, 938.
(43) Ajayan, P. M.; Tour, J. M. *Nature* **2007**, 447, 1066.
(44) Kukovecz, A.; Kónya, Z.; Nagaraju, N.; Willems, I.; Tamási, A.; Fonseca, A. *Phys. Chem. Chem. Phys.* **2000**, 2(7), 3071.
(45) O'Connell, M. J.; Boul, P.; Ericson, L. M.; Huffman, C.; Wang, Y.; Haroz, E.; C. Kuper, C.; Tour, J.; Ausman, K. D.; Smalley, R. E. *Chem. Phys. Lett.* **2001**, 342, 265.

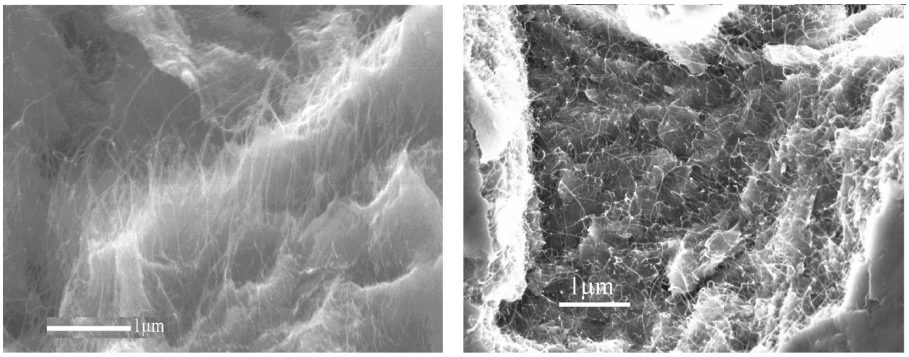

Figure 1. Scanning electron microscopy images of (a) single-walled and (b) multiwalled carbon nanotubes dispersed in aqueous PSS solution. Images taken after drying a few drops of the dispersions on pieces of silicon.

electron microscopy images of PSS based dispersions of single- and multiwalled nanotubes, depicting bundle sizes of 20−40 nm for SWNTs and 15−30 nm for MWNTs. Measured amount of CNT-PSS dispersion was then added, using a pipet, to the surface of a 20 wt % aqueous solution of polydiallyldimethylammonium chloride (PDDA) without disturbing the interface of the PDDA solution and nanotube dispersion. Because of high ionic interaction between oppositely charged PSS and PDDA, the dispersion instantaneously formed an insoluble precipitated complex at the interface, as shown in Figure 2b. The complex formed on the surface could be picked up using a pair of tweezers and manually drawn resulting in a fibrous structure, as shown in Figure 2c. The fibers were then allowed dry in an oven at a temperature of 120 °C for 30 min. The fibers collapsed as ribbons if dried on a flat surface but retained the fibrous structure upon drying as freely suspended fibers, shown in Figure 2d. The order of addition of polyelectrolytes (bulk vs solute phase) does not matter for interfacial precipitate formation, however the fiber formation process via drawing is influenced by the properties, especially viscosity and molecular weight, of the bulk polyelectrolyte. Although the low molecular weight and hence lower viscosity of PSS is more suitable for forming aqueous dispersions that can stabilize nanotubes with relative ease, the higher molecular weight and higher viscosity solution of PDDA is more suitable to be the bulk phase in the fiber drawing and formation process. Hence, although the addition of PDDA (cationic polymer) to the PSS−nanotube dispersion (anionic polymer) does lead to formation of a thin film precipitate at the interface, it cannot be easily drawn into fiber form.

The order of addition (bulk vs solute phase) depends on relative viscosities and molecular weights of the polyelectrolytes involved. Although the low molecular weight and lower viscosity of PSS was more suitable for dispersing nanotubes in aqueous solution, higher molecular weight and higher viscosity PDDA solution was more suitable as a bulk phase for fiber drawing and synthesis process.

It should be noted that dispersions without nanotubes (polyelectrolyte precipitate only) and those containing 0.1 wt % carbon nanotubes could not be easily drawn into fiber form, as they were very weak and usually broke

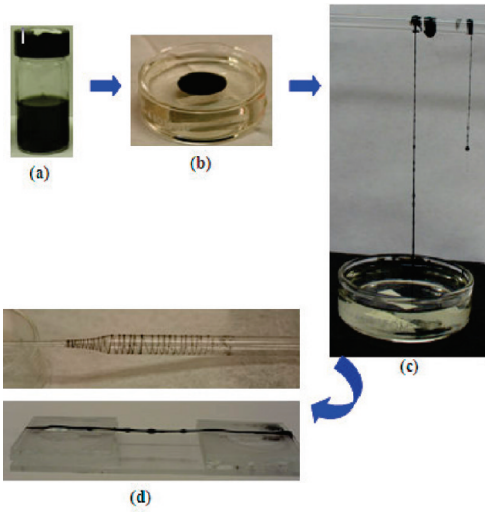

Figure 2. Schematic of the steps involved in the formation of CNT polyelectrolyte complex fibers. (a) PSS/SWNT dispersion, (b) precipitate of PSS/SWNT formed on the surface of PDDA (transparent solution), (c) manual drawing of fibers using a glass rod, and (d) collecting and drying fibers on flat surfaces or as freely suspended fibers.

either during the drawing process or during drying. This could be due to weak mechanical strength of the polyelectrolyte precipitate as well as not enough threshold viscosity of the precipitated mass to pull the mass into fiber form. Moreover, 0.1 wt % nanotube content might not be sufficient to provide appropriate mechanical stability, thereby leading to the formation of weaker fibers that break easily. Thus, most of the characterization studies, especially those involving mechanical properties of the fibers, were carried out on 0.5 and 1 wt % dispersions of carbon nanotubes, which were relatively strong, easy to handle, and could be drawn into long lengths easily. A PSS/PDDA complex precipitate film was used as a control sample for mechanical testing. When initially drawn from the polyelectrolyte complex interface, the fibers had small beads that could be the solvent-rich polymer masses not fully stretched during fiber drawing. The beads on the fiber surface usually collapsed and disappeared upon drying (see Figure S1 in the Supporting Information). Using a motorized spinning process, as shown in Figure 3, fibers in the diameter range of

100−150 μm were produced (much shorter fiber lengths of smaller diameters ~10 μm could also be produced via slower manual drawing using tweezers). The length of the fibers was limited only by the amount of precipitate formed (depending on initial amount of CNT dispersion added) and the drawing process. The fibers produced were tough, easy to handle, and pliable enough to be tied into knots. Scanning electron microscopy images of the fibers showed a scaly outer surface, as shown in Figure 4a, which indicates similarity with other polyelectrolyte fibers reported in previous literature.[17,18] A number of impurity aggregates were observed on the surface as well, running throughout the length of the fiber. At the cross-section of the polyelectrolyte fiber, well-dispersed nanotubes could be seen protruding from the surface, as shown in Figure 4b. This dense network of nanotubes runs throughout the body of the fiber, giving it structural integrity, mechanical strength, and electrical conductivity.

Having optimized the fiber synthesis process for the PSS/PDDA system, other strong polyelectrolyte systems were also used to form fibers via the polyelectrolyte complexation process, such as chitosan being the cationic polyelectrolyte and poly (L-glutamic acid) (PLG) as the anionic polyelectrolyte. Both SWNT and MWNTs were used to prepare these fibers. One of the most important and useful system used was the PEDOT: PSS polymer conjugate acting as the anionic polyelectrolyte and PDDA as the cationic polyelectrolyte. Using PEDOT provided a conducting polymer matrix that is proposed to have significant effects on the electrical properties of the resulting fibers. To prepare these fibers, single-walled carbon nanotubes were dispersed in a 1.3 wt % solution of the PEDOT:PSS conjugate polymer system, using a successive ultrasonication technique similar to that described earlier. This dispersion was then added to a 20 wt % PDDA solution in water, as the cationic base polymer. A thin precipitate layer was immediately formed on the surface of PDDA, which just like earlier cases could be spun into long fibers. An interesting outcome of this experiment was that we were able to synthesize control PEDOT/PSS/PDDA fibers as well (without nanotubes), in addition to fibers containing embedded carbon nanotubes.

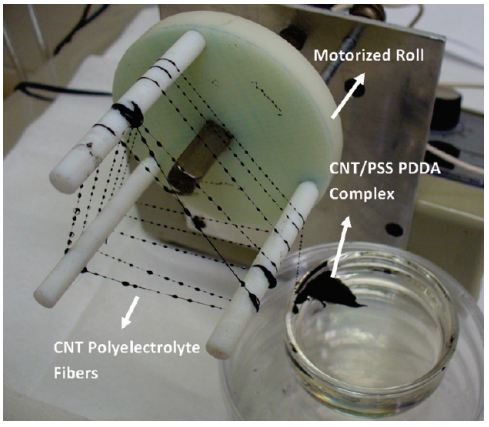

Figure 3. Continuous fiber drawing apparatus used for drawing and collecting CNT polyelectrolyte complex fibers. Note the presence of beads on the surface of wet fibers.

3.2. Fiber Formation Process. Previous research into formation of polyelectrolyte complex (PEC)-based fibers has shown the mechanism of fiber formation to be a multistep process.[18] The first step is the formation of a polyelectrolyte complex film at the interface of two oppositely charged polymers, which when drawn leads to the formation of micrometer-sized "nuclear fibers". These "nuclear fibers" further coalesce to form thicker fibers along with formation of "beads" or coagulated gels at regular intervals along the length of the fiber that collapse during drying.[18] These fibers, when viewed under a scanning electron microscope, possess a scaly outer structure thought to result from coalescing of multiple such micrometer-sized nuclear fibers.[18] To establish this in the case of SWNT/PSS/PDDA complex fiber synthesis, optical microscopy was performed at a 100× magnification during the fiber drawing process, depicted in Figure 5.

The drawn fiber in its wet state comprises of various small "nuclear" fibers forming the body of a larger thicker fiber, as shown in Figure 5a. A surrounding "shell" of PDDA polymer can also be seen in the image, contributing to fiber formation via complexation. The second part of the figure shows a bunch of the small nuclear fibers coalescing together at the air/polymer interface to form a bigger fiber. Several individual polyelectrolyte complex

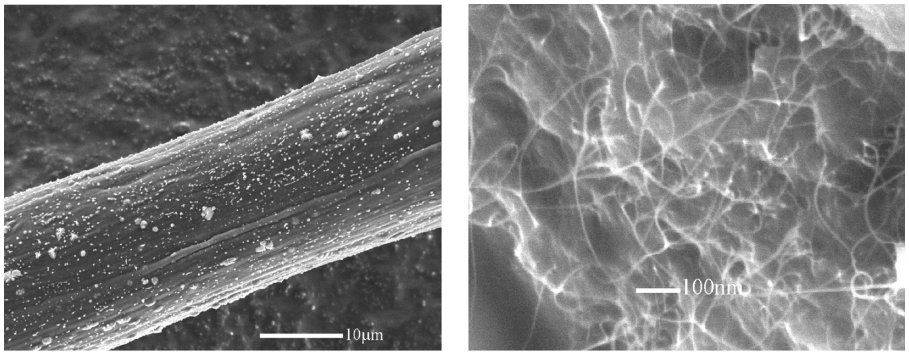

(a) (b)

Figure 4. Scanning electron microscopy images of (a) fiber surface (notice surface impurities), and (b) fiber cross-section showing protruding nanotubes.

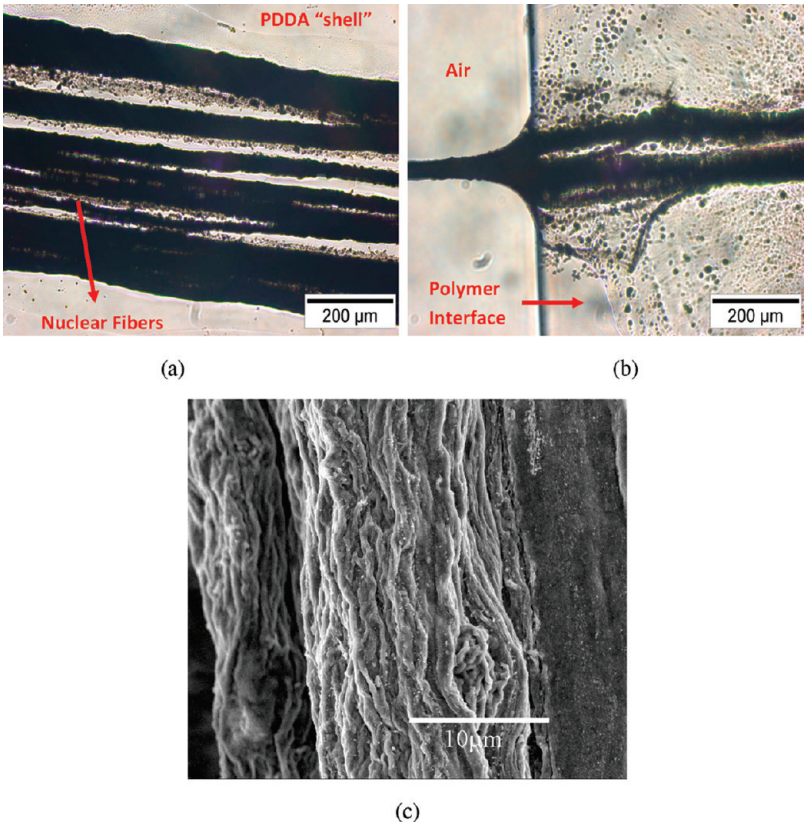

Figure 5. Optical microscopy images depicting (a) surface of a recently drawn wet CNT/PEC complex fiber, (b) drawn fiber at the air/polymer complex interface (100× magnification), and (c) scanning electron microscopy image of the scaly surface of the shown fiber after drying.

(PEC) particles are also found to be dispersed randomly across the polymer matrix. The scanning electron microscopy images of the resulting SWNT polyelectrolyte complex fiber, such as shown in Figure 5c show a scaly surface like that observed in previous polyelectrolyte complexes.[18]

During the fiber drawing process, it was observed that the fibers could be gently treated or "washed" with water so as to remove any extraneous impurities on the surface of the fiber. The process involved pouring a gentle stream of water on the fibers held in a vertical position for about 10 s which was observed to remove most of the surface impurities. Energy-dispersive X-ray spectroscopy (EDS) used in conjunction with SEM showed the presence of sodium chloride (NaCl) based impurities on the fiber surface, formed as a byproduct of the complexation reaction, and confirmed the removal of such impurities from the fiber surface upon water treatment, shown in Figure 6. The water treatment or "washing" of the fibers also resulted in partial removal of the soluble polymer matrix shell, which in turn was observed to lead to densification of the embedded nanotube network, as depicted in Figure 7. This, as discussed in subsequent sections, was seen to have a profound effect on the electrical and mechanical properties of the fiber.

FTIR spectroscopy performed for SWNT/PEC fibers also delineated this difference in composition for pristine vs washed fibers, as shown in Figure 8. The FTIR spectrum shows characteristic absorption bands of PSS and PDDA. The broad absorption band at ~3520 cm^{-1} corresponds to the presence of moisture in the sample. Absorbance bands at 2100 and 1640 cm^{-1} correspond to amine group based on $NR_4^+Cl^-$ type linkages present in PDDA.[46] The region from 1500 to 1100 cm^{-1} consists of a multitude of small bands belonging to the PSS structure. For example, the absorption bands at 1490 and 1413 cm^{-1} correspond to the stretching vibration of the C−C bonds in an aromatic ring, present in the PSS structure.[47] There is also a broadband in the region of 1190 cm^{-1} belonging to S=O stretching vibrations. The intensities for both polymers, especially PDDA, which forms the outer polymer shell, are significantly reduced for the washed fibers. The intensity for the 2100 cm^{-1} band was reduced by more than half, whereas the 1640 cm^{-1} band almost disappeared. For PSS, the 1490 and 1413 cm^{-1} bands are replaced by a generic broader peak, whereas the broad absorbance region at 1190 cm^{-1} was replaced by a new band at ~1240 cm^{-1}, which may belong to C−O stretching modes of carboxylic acid groups, being visible due to lower intensities of neighboring bands. Washing of SWNT/PEC fibers was thus observed to be an important step to control and manipulate the synthesis process in order to improve or enhance the physical properties of the resulting fiber, delineating the structure−property relationship of the embedded nanotube network interacting with the polyelectrolyte matrix.

(46) Lu, J.; Zhang, J.; Xiao, C. *J. Appl. Polym. Sci.* **2007**, 106, 1972.
(47) Ge, L.; Pan, C.; Chen, H.; Wang, X.; Wang, C.; Gu, Z. *Colloids Surf., A* **2007**, 293, 272.

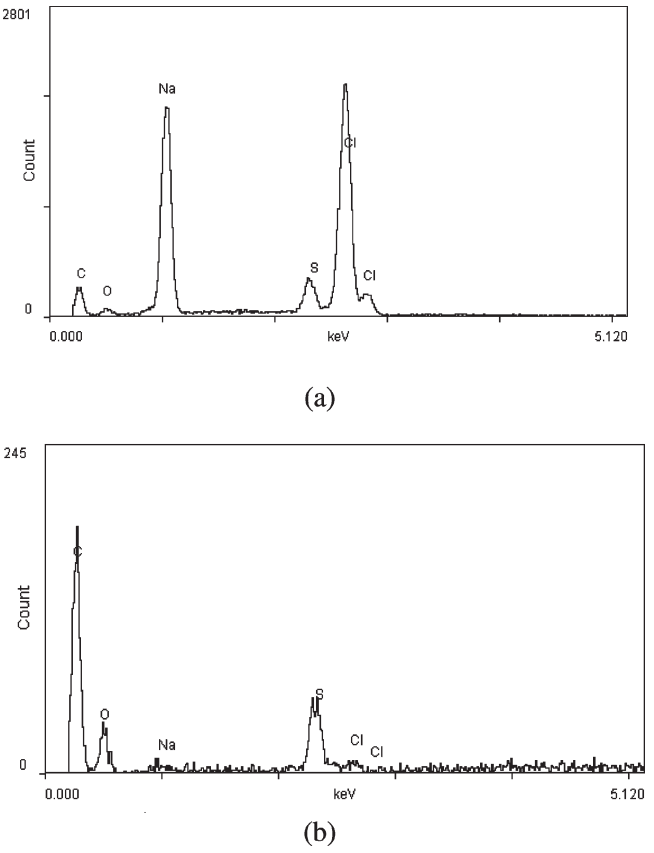

Figure 6. EDS spectra for (a) unwashed fiber surface with impurities showing a high presence of Na and Cl and (b) washed fiber surface with low levels of Na and Cl and higher amounts of C and S due to nanotubes and PSS polymer.

3.3. Fiber Properties. Uniaxial tensile testing was carried out on the fibers in order to investigate fiber strength as a function of synthesis parameters. Figure 9 depicts the engineering stress−strain curves obtained for 0.5 and 1 wt % concentrations of SWNT in PSS, including comparative tensile curves for the respective washed fibers.

Higher concentrations of nanotubes on average resulted in higher values of tensile strengths (TS), Young's modulus and strain-to-break. This becomes intuitive considering the network of nanotubes embedded inside the polymer matrix providing structural integrity and mechanical strength to the fibers. The tensile strength of washed fibers was observed to be almost twice as high as the unwashed fibers, indicating a possible effect of nanotube densification upon washing, as discussed earlier.

Fiber fracture surfaces studied via scanning electron microscopy were found to be quite brittle and smooth, as shown in Figure 10. The fracture surfaces also showed presence of a large amount of surface impurities with crack propagation initiated along microcracks running in an orthogonal direction to the applied tensile stress direction.

Using MWNTs, higher tensile strength (~70 MPa) and Young's modulus (3.8 GPa) values were obtained (TS for 0.5 wt % being ~40 MPa with a Young's modulus of 3.2 GPa) compared to SWNT based fibers (see Figure S2 in the Supporting Information). Thus, both tensile strength and Young's modulus for MWNT based fibers were, on average, a factor of 3−4 times higher than their SWNT counterpart, for the same polyelectrolyte systems and synthesis conditions used. Because there is not a significant difference between the theoretical tensile strength and Young's modulus of single-walled and multiwalled carbon nanotubes,[48] this difference in fiber strength could be attributed to a higher level of interaction between MWNTs with PSS, as PSS acts as a glue and interacts both with nanotubes and the PDDA polymer. Better interaction of MWNTs with PSS could be traced back to better dispersions of MWNTs in PSS as well as a smaller particle size, as compared to SWNTs. One of the possible reasons for better interaction and dispersibility of MWNTs could arise from bigger diameters and thus smaller curvature of MWNTs, making it easier for polymer chains to wrap around their surface compared to SWNTs. Although no experimental or modeling results are presented to validate the above-mentioned hypothesis, it might be one of the factors affecting the distribution of PSS around MWNTs and consequently the properties of the fiber itself.

Tensile testing was also performed on other polyelectrolyte fiber systems using MWNTs, with the corresponding data detailed in Figures S2 and S3 and Table 1 in the Supporting Information). The choice of polyelectrolyte system used seems to modulate fiber strength and Young's modulus to some extent, however, nanotube concentration and their interaction with the base polymer system seem to be major contributors toward mechanical properties of the resulting fiber. This also explains higher tensile strengths and Young's modulus obtained for "washed" fibers where nanotube densification greatly influences the mechanical strength of the fiber, possibly because of greater interaction between the reinforcing nanotubes (higher number of nanotube junctions), leading to stronger fibers.

Electrical properties of the fibers also show a similar trend, where the presence of an interconnected nanotube network influences the electrical conductivity of the nanotube−polyelectrolyte complex fiber. The effect of nanotube addition and densification due to "washing" on the electrical conductivity of the fibers was investigated by calculating the four-probe resistivities of the different fibers, as shown in Figure 11. About 1 order of magnitude difference was observed in the conductivity of 0.5 wt % (2 S/cm) vs 1 wt % (20 S/cm) single-walled carbon nanotube based complex fibers. Overall, four probe resistivity measurements revealed higher values of conductivity with increasing carbon nanotube concentration in the original dispersion. Densification of nanotubes as a result of water treatment of fibers during synthesis also seemed to influence the conductivity of the resulting fibers. For the same concentration of nanotubes, two- to four-fold enhancements in conductivities were obtained for both 0.5 wt % and 1 wt % nanotube addition upon washing. Scanning electron microscopy images taken from longitudinal sectioning of the fiber show such a dense interconnected network running across the fiber length, as depicted in Figure 12.

(48) Dresselhaus, M. S.; Dresselhaus, G.; Saito, R. *Carbon* **1995**, 33(7), 883.

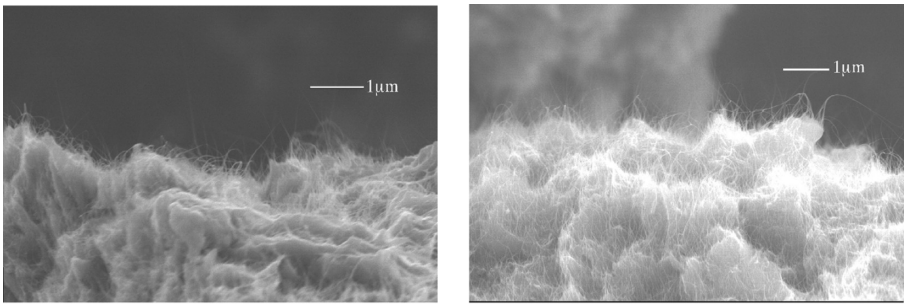

Figure 7. Cross-sectional scanning electron microscopy images of 0.5 wt % SWNT/PSS/PDDA fibers, with (a) depicting cross-section of unwashed fiber and (b) cross-section of a "washed" fiber showing denser packing of nanotubes at the surface (larger amount of nanotubes in a given area).

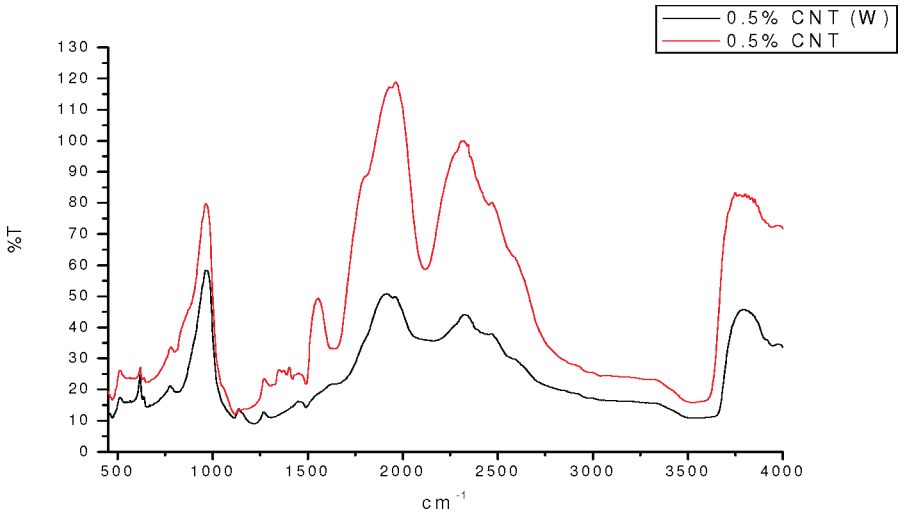

Figure 8. Comparative FTIR spectra for washed and pristine 0.5 wt % SWNT/PSS/PDDA fiber.

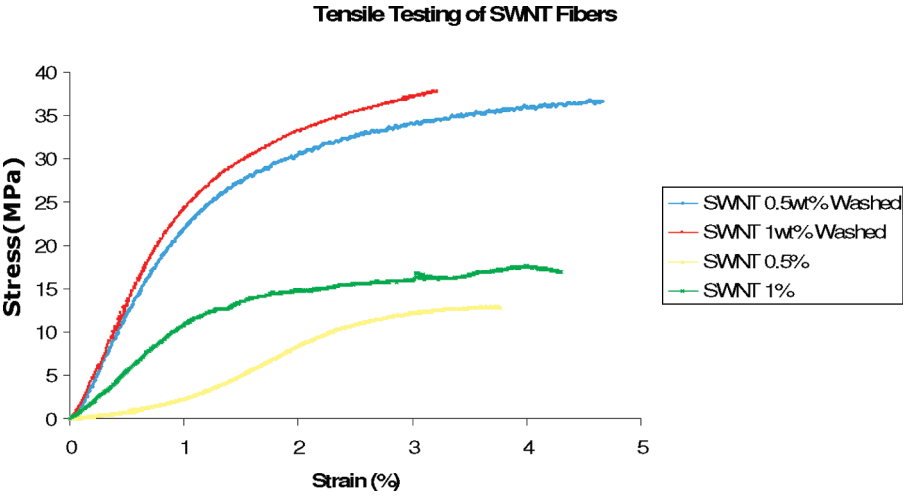

Figure 9. Comparative engineering stress−strain curves for SWNT/PSS/PDDA fibers with different concentrations and water pretreatments.

Overall, conductivity values of around 45 S/cm were observed for water treated 1 wt % SWNT/PSS/PDDA fibers. This value is about 2 orders of magnitude higher than the polymer-based coagulation spinning method.[49]

Much higher values of 35−40 S/cm and 75−90 S/cm were obtained for 0.5 and 1 wt % MWNT-based complex fibers respectively. In fact, the values of conductivity obtained for both SWNT and MWNT are one of the highest reported in literature for a nonconducting polymer/SWNT composite fiber, except for fibers obtained from a highly conducting polymer matrix with a

(49) Vigolo, B.; Penicaud, A.; Coulon, C.; Sauder, C.; Pailler, R.; Journet, C.; P. Bernier, P.; Poulin, P *Science* **2000**, 290, 1331.

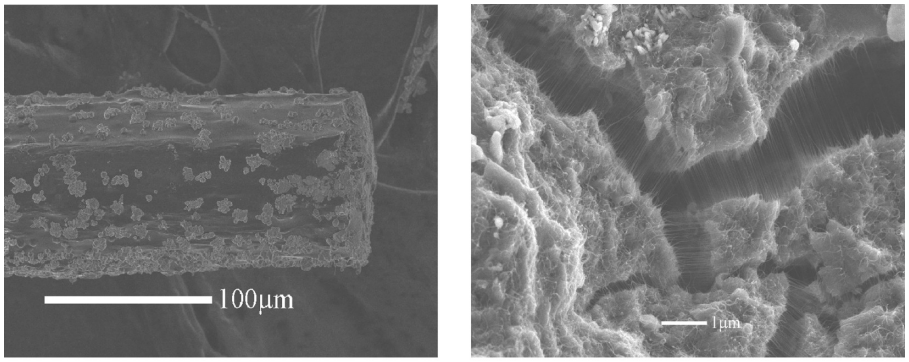

Figure 10. Scanning electron microscopy images of (a) side view of the fractured fiber showing a brittle surface and (b) top view of the fracture surface showing the presence of micrometer-sized cracks running across the surface, with aligned nanotubes across the interface.

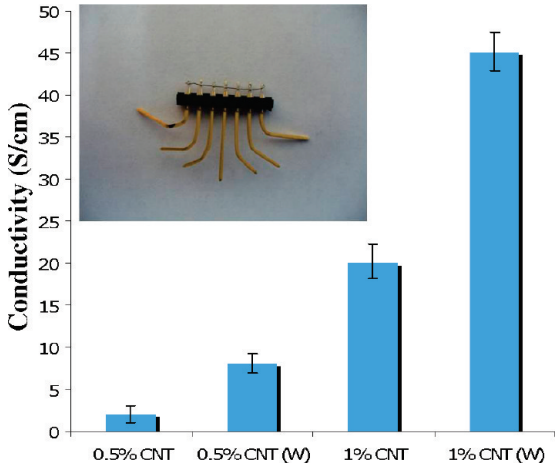

Figure 11. Graph showing conductivity values of fibers obtained from different concentrations of nanotube dispersions, with (W) representing the "washed" fibers (inset showing device used for four probe measurements).

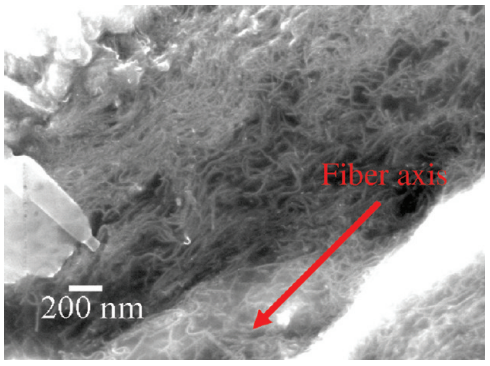

Figure 12. Scanning electron microscopy image of a longitudinal fiber section showing distribution of nanotubes across fiber length.

significantly high value of conductivity before nanotube addition (such as for nanotube addition to a polyaniline matrix).[50] This gave an indication toward the intimate interaction of the polymer phase with the nanotubes distributed throughout the fiber matrix. PSS here acts as a binding agent, with the nonpolar part wrapped

(50) Mottaghitalab, V.; Spinks, G. M.; Wallace, G. G. *Polymer* **2006**, 47, 4996.

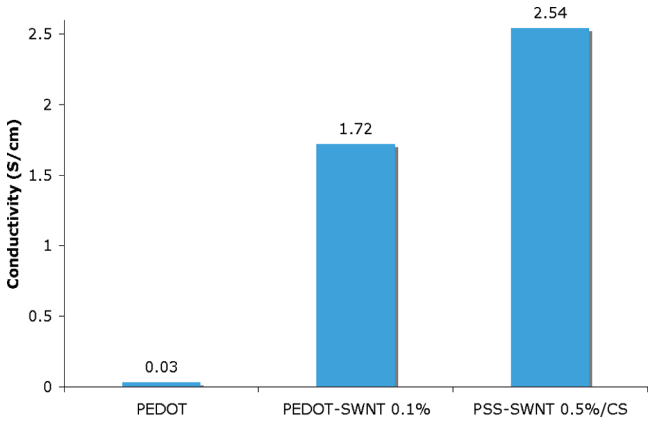

Figure 13. Comparative conductivity values of fibers obtained using different polyelectrolyte systems, viz. PEDOT fibers, PEDOT/SWNT/PDDA fibers, and SWNTPSS/chitosan fibers.

around nanotube surface and polar part interacting with oppositely charged polyelectrolyte.

In case of PEDOT-based fibers, given an already conducting polymer matrix, presence of carbon nanotubes further enhances the conductivity of the resulting fiber by 2 orders of magnitude, as shown in Figure 13. This indicated a synergistic relation between the two conducting materials present in the fiber structure, with PSS (the dopant for PEDOT dispersion) acting as "glue" between the conducting PEDOT matrix and carbon nanotubes.

To determine the actual amount of nanotubes by weight in the polyelectrolyte complex fibers, thermogravimetry was performed on pristine nanotubes, polyelectrolyte complex of PSS, and PDDA (without nanotube presence), and SWNT/PSS/PDDA fibers. Figure 14 shows comparative thermograms for control samples of SWNT, PSS/PDDA complex, and SWNT-based PSS/PDDA fibers. We estimated the residues for the control samples as well as for the fiber at 1000 °C using TGA. The percentage of nanotubes by weight was estimated, based on residue, to be ~12 wt % for 0.5 wt % SWNT dispersion-based fiber, and ~20 wt % for 1 wt % SWNT dispersion-based fiber.

3.4. Fiber Applications. Aligned carbon nanotube structures have been studied in previous literature as potential field emitters.[52] The small size, high aspect ratio,

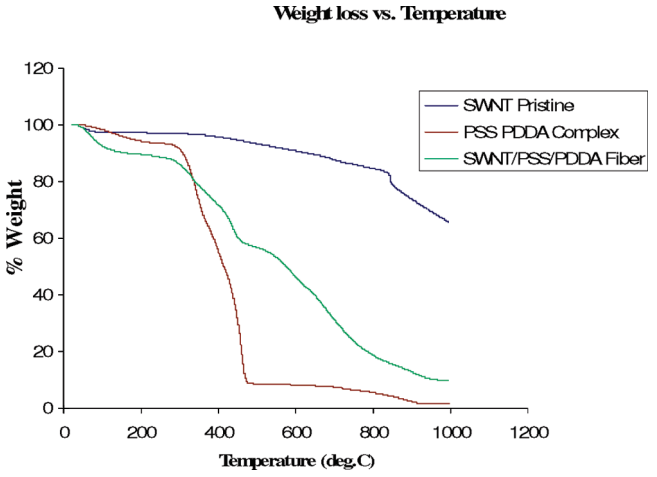

Figure 14. Thermogravimetry curves for pristine SWNT (in powder/particle form), PSS/PDDA complex (thin film precipitate without nanotubes) and 0.5 wt % SWNT/PSS/PDDA fibers (drawn fibers from complex formed from 0.5 wt % SWNT-PSS dispersion & PDDA precipitation).

small radius of curvature at the tips, high chemical stability, and high mechanical strength make carbon nanotubes ideal candidates for field-emission applications. In case of nanotubes, field emission occurs when the enhanced electric field around the tip of nanotubes becomes greater than the work function of the nanotubes, leading to a tunneling current flowing across two electrodes.[52]

In our study, protruding nanotubes present at the cross-section of brittle fiber fracture surfaces presented architectures that could be suitable for field-emission applications. Figure 15 depicts a typical cross-section of an ~15 μm fiber synthesized from SWNTs using PSS/PDDA complexation process. Well-aligned protruding nanotubes can be seen at the fiber cross-section, and because the fiber itself had reasonable conductivity, the fibers could be attached to a voltage source and tested as a field-emission device.[51]

Figure 16 shows an $I-V$ plot obtained for a 0.5 wt % SWNT/PSS/PDDA fiber showing emission behavior. The inset depicts the measured data plotted fitting a Fowler–Nordheim expression,[52] which is used to describe characteristics of field emission behavior, demonstrating successful field emission occurring from the fiber cross-section. A turn-on electric field of ca. 14 V μm^{-1} was obtained for the fiber, considering the minimum detectable change in field current by the measuring device was around 1 nA. By measuring the slope of

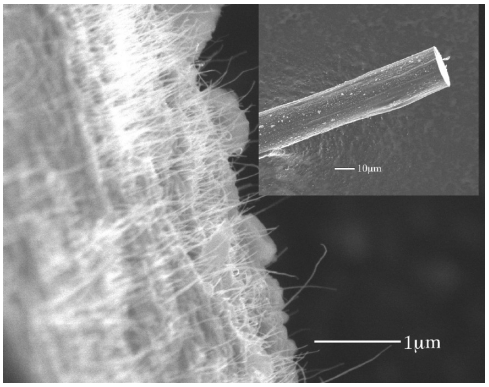

Figure 15. Scanning electron microscopy image of SWNT polyelectrolyte complex fiber cross-section, with inset showing the low-magnification image of fiber surface and cross-sectional edge.

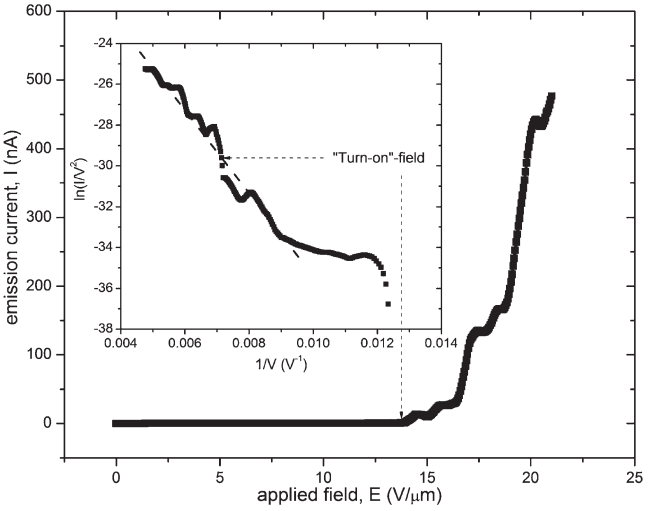

Figure 16. Current vs electric field data plotted for a SWNT/PSS/PDDA fiber. The inset shows a Fowler–Nordheim plot of the relevant data showing field emission.

the Fowler–Nordheim plot, the field enhancement factor, β, was calculated to be 1354. A current density of 1.59 mA/cm^2 was observed for an applied electric field of around 20 V μm^{-1}. Thus, the fibers seemed to exhibit reasonable field emission behavior that could be useful for appropriate applications. Besides the field emission behavior shown here, these fibers could also be useful for a number of applications such as chemical and biological sensors, electrochemical electrodes, filtration membranes, etc., because of their layered ionic composition, flexible structure that can be used as fibers or woven into sheets, and high conductivity values.

4. Conclusion

Carbon nanotube fibers were synthesized from an ionically assembled polyelectrolyte precipitate using noncovalent stabilization of carbon nanotube aqueous dispersion. A simple fiber formation technique was demonstrated from the self-assembled polyelectrolyte precipitate and carbon nanotube combination where no functionalization of the nanotubes was necessary. The role of carbon nanotubes and their interactions with the

(51) To carry out field emission measurements, we mounted short lengths (~5 mm) of fiber in a normal direction on a metallic base using silver paint and kept them at a distance ~30 μm a part from another metallic base. The assembly was then placed in a vacuum chamber, where field emission measurements were carried out at room temperature and pressure of ~1 × 10^{-6} Torr. The values of current passing between the two metallic bases was measured as a function of a range of voltages applied, with the upper limit being restricted to 210 V due to the limitations of the measuring device (Keithley 2400 Sourcemeter).

(52) Jung, Y. J.; Kar, S.; Talapatra, S.; Soldano, C.; Viswanathan, G.; Li, X.; Yao, Z.; Ou, F. S.; Avadhanula, A.; Vajtai, R.; Curran, S.; Nalamasu, O.; Ajayan, P. M. *Nano Lett.* **2006**, 6, 413.

polyelectrolytes during complex precipitate formation was addressed that has not been studied previously. The polyelectrolyte−carbon nanotube fiber composite systems show interesting electrical, chemical, and mechanical properties. Such systems of polyelectrolyte complex fibers containing carbon nanotubes are promising for a variety of applications such as biosensors, chemical electrodes, and flexible electronics where the combination of flexibility as well as high conductivity is required.

Acknowledgment. P.M.A. and S.K. thank the interconnect focus center, RPI, Troy, NY for this research.

Supporting Information Available: Time-lapse optical microscopy images of a bead collapsing on the surface of 0.5 wt % SWNT-PSS/PDDA polyelectrolyte fiber. Engineering stress−strain curves of MWNT based fibers for different polyelectrolyte systems (comprising of various combinations of strong polyanion and polycations. Table showing mechanical properties of fibers obtained from different polyelectrolyte systems (PDF). This material is available free of charge via the Internet at http://pubs.acs.org.